INFECTION AND IMMUNITY, Apr. 2000, p. 2315–2322 Vol. 68, No. 4
0019-9567/00/$04.00+0

Cryptosporidium parvum Induces Host Cell Actin Accumulation at the Host-Parasite Interface

DAVID A. ELLIOTT AND DOUGLAS P. CLARK*

Department of Pathology, The Johns Hopkins University School of Medicine, Baltimore, Maryland 21287

Received 1 November 1999/Returned for modification 29 November 1999/Accepted 11 December 1999

***Cryptosporidium parvum* is an intracellular protozoan parasite that causes a severe diarrheal illness in humans and animals. Previous ultrastructural studies have shown that *Cryptosporidium* resides in a unique intracellular compartment in the apical region of the host cell. The mechanisms by which *Cryptosporidium* invades host intestinal epithelial cells and establishes this compartment are poorly understood. The parasite is separated from the host cell by a unique electron-dense structure of unknown composition. We have used indirect immunofluorescence microscopy and confocal laser scanning microscopy to characterize this structure. These studies indicate that host filamentous actin is assembled into a plaque-like structure at the host-parasite interface during parasite invasion and persists during parasite development. The actin-binding protein α-actinin is also present in this plaque early in parasite development but is lost as the parasite matures. Other actin-associated proteins, including vinculin, talin, and ezrin, are not present. We have found no evidence of tyrosine phosphorylation within this structure. Molecules known to link actin filaments to membrane were also examined, including α-catenin, β-catenin, plakoglobin, and zyxin, but none was identified at the host-parasite junction. Thus, *Cryptosporidium* induces rearrangement of the host cell cytoskeleton and incorporates host cell actin and α-actinin into a host-parasite junctional complex.**

Cryptosporidium parvum is an intracellular protozoan parasite that is an important cause of diarrheal illness worldwide (7). Humans are susceptible hosts in a variety of settings including people with AIDS, children in developing countries, and immunocompetent hosts of waterborne illness. Despite the medical importance of this infection, the pathogenesis is poorly understood (4).

Cryptosporidiosis is initiated when a host ingests oocysts from the environment. Once in the bowel, these oocysts release sporozoites, which rapidly invade the epithelial cells lining the intestines. There, the parasite completes both the asexual and sexual phases of its life cycle. During the invasion process *Cryptosporidium* establishes a unique intracellular compartment within the host cell in which it divides. This unique compartment has been termed intracellular but extracytoplasmic, since it appears to be separated from the apical host cell cytoplasm and bulges into the lumen of the gut (Fig. 1) (28).

During *Cryptosporidium* invasion and intracellular development, several elements of host cell cytoskeleton appear to be disrupted. First, the microvilli which normally cover the intestinal epithelial cell are absent in the area of parasite invasion (18, 21). Second, the normally columnar epithelial cells are often significantly shortened after invasion by *Cryptosporidium* (15, 19). Third, a unique structure is formed at the host-parasite interface during invasion, containing an electron-dense band of unknown composition and an adjacent filamentous network (Fig. 1) (18, 21, 29). We have undertaken this study to better understand the cytoskeletal changes that occur in *Cryptosporidium*-infected cells.

* Corresponding author. Mailing address: The Johns Hopkins Hospital, 406 Pathology Building, 600 N. Wolfe St., Baltimore, MD 21287. Phone: (410) 955-1180. Fax: (410) 614-9556. E-mail: dclark@mail.jhmi.edu.

MATERIALS AND METHODS

Experimental murine infections. BALB/c mouse pups were infected with approximately 5,000 oocysts (AUCp-1 isolate) at 48 h of age and sacrificed 72 h later. Small intestinal tissue was harvested and fixed in 4% paraformaldehyde plus 1% glutaraldehyde. The tissue was postfixed in osmium tetroxide for 1 h and embedded in Epon. Sections of 80 nm were cut, and transmission electron photomicrographs were obtained using a Hitachi H-600 electron microscope.

Experimental infection of HCT-8 cells. The human colonic adenocarcinoma cell line HCT-8 (ATCC CCL-244) was purchased from the American Type Culture Collection (ATCC; Manassas, Va.) and grown according to ATCC instructions on 22-mm^2 glass coverslips in six-well plates. Confluent HCT-8 cells were infected with 2×10^5 *C. parvum* oocysts/well (Iowa isolate; Pleasant Hill Farm, Troy, Idaho) 24 h after plating on glass coverslips. When indicated, intracellular parasites were hypotonically extracted from host cells by gently washing cells in phosphate-buffered saline (PBS), incubating them on ice for 2 min, dipping coverslips in distilled H_2O for 10 s, incubating cells in PBS for 5 min, and then fixing cells as described below. This hypotonic extraction is a modification of a protocol provided by Margaret Perkins, Columbia University.

Culture of GFP-actin-expressing cell line. The cells and their culture methods have been previously published (25). Briefly, clone A10 is a Madin-Darby canine kidney (MDCK) clone expressing human cytoplasmic (i.e., nonmuscle) β-actin fused in frame with the enhanced green fluorescent protein (GFP) gene in the Clontech pEGEP-C1 vector. The clone was cultured in low-glucose Dulbecco modified Eagle medium with 10% fetal bovine serum, antibiotics, and Geneticin (G418; 300 μg/ml). Three days before experiments were performed, the medium containing G418 was replaced with G418-free medium. Cells were maintained in 10-cm plates in 5.5% CO_2 at 37°C and subcultured 1:5 when confluent.

Fluorescence microscopy. In preparation for staining, 24 h postinfection HCT-8 cell monolayers were washed in PBS, fixed for 10 min in 3.7% formaldehyde (J. T. Baker, Phillipsburg, N.J.), washed again, and permeabilized for 10 min in 0.1% Triton X-100 (Sigma, St. Louis, Mo.). The monolayers were then blocked for 10 min in 1% bovine serum albumin (BSA; Sigma) and incubated for 45 min with primary antibody plus 4,′6′-diamidino-2-phenylindole dilactate (DAPI; 5 μg/ml; Molecular Probes, Eugene, Oreg.), 1% BSA, and 3% goat serum (Sigma) in PBS. Monolayers were then washed in blocking solution and incubated for 30 min with secondary antibody and fluorescein isothiocyanate (FITC)-phalloidin (5 μg/ml; Sigma) or tetramethylrhodamine B isothiocyanate-phalloidin (5 μg/ml; Sigma) plus 1% BSA and 3% goat serum in PBS. Monolayers were then washed again, postfixed with 3.7% formaldehyde, and mounted. Negative controls omitted the primary antibody. The following antibodies (each monoclonal unless indicated otherwise) were used: antiactin (polyclonal, against a 13-amino-acid N-terminal actin peptide; A5060; Sigma), 1:200; anti-α-actinin (A5044; Sigma), 1:200; anti-α-catenin (C21620; Transduction Laboratories, Lexington, Ky.), 1:250; anti-β-catenin (13-8400; Zymed, San Francisco, Calif.), 1:200; antiezrin (E53020; Transduction Laboratories), 1:250; antikeratin AE1/AE3 (1124 161; Boehringer Mannheim, Indianapolis, Ind.), 1:2,000;

FIG. 1. Transmission electron micrograph of a murine small intestinal epithelial cell infected by *Cryptosporidium*. Note the electron-dense band (arrow) separating the parasite from the host cell cytoplasm and the filamentous network immediately beneath this structure (brackets). Magnification, ×15,000.

anti-mouse-Cy3 (711-165-152; Jackson ImmunoResearch Laboratories, West Grove, Pa.), 1:250; anti-pan-tubulin rabbit antiserum (a gift from Doug Murphy), 1:50; antiphosphotyrosine (03-7700; Zymed), 1:200; antiplakoglobin (C26220; Transduction Laboratories), 1:400; anti-rabbit-Cy3 (711-165-152; Jackson ImmunoResearch Laboratories), 1:250; anti-rat-FITC (712-095-150; Jackson ImmunoResearch Laboratories), 1:250; antitalin (T3287; Sigma), 1:40; antivillin (V34420; Transduction Laboratories), 1:100; antivimentin (18-0052; Zymed), 1:50; antivinculin (V9131; Sigma), 1:400; and antizyxin (Z45420; Transduction Laboratories), 1:2,000.

Fluorescence microscopy was performed with a Zeiss Axiovert 135TV equipped with a Photometrics PXL-1400 CCD camera. Images were histogram stretched, and the camera and microscope were controlled with IPLab Spectrum 3.1. Confocal micrographs were obtained using an inverted Zeiss LSM 410 confocal microscope with a Zeiss C-Apo 40× water objective. Final image manipulations were performed using Adobe Photoshop 5.0.

RESULTS

Phalloidin staining of *Cryptosporidium*-infected cells revealed filamentous actin accumulation at the host-parasite interface. FITC-phalloidin staining of a *Cryptosporidium*-infected cell line revealed striking accumulation of filamentous actin (f-actin) at every focus of parasite invasion. As shown in Fig. 2B and E, this accumulation appeared as a circumscribed, circular, plaque-like collection of actin filaments. At early stages of parasite development (trophozoite stage), which contain a single nucleus, the actin plaque measured approximately 3 μm in diameter and had a central point of intense staining surrounded by less intense, homogeneous staining (Fig. 2B). Further in development, after nuclear division had occurred (meront stage), the f-actin accumulation was larger (approximately 5 μm in diameter), had lost the intense central point of staining, and instead appeared homogeneous (Fig. 2B and 2E). This homogeneous staining pattern strongly suggests that the structures being stained are not within the individual parasites, since staining of the two to eight organisms present at the meront stage would produce a more complex pattern within the meront. FITC-phalloidin staining of extracellular merozoites is much less intense than the actin plaque staining (data not shown). Utilizing a protocol employing brief exposure of the infected monolayer to a hypotonic solution, we removed many of the intracellular parasites from the host cells, leaving behind vacant compartments on the host cell surface visible by differential interference contrast (DIC) microscopy (Fig. 2C). Host cells subjected to this protocol lost intracellular parasites (as demonstrated by lack of DAPI-stained parasite nuclei [Fig. 2D]) but retained the FITC-phalloidin-stained f-actin plaque

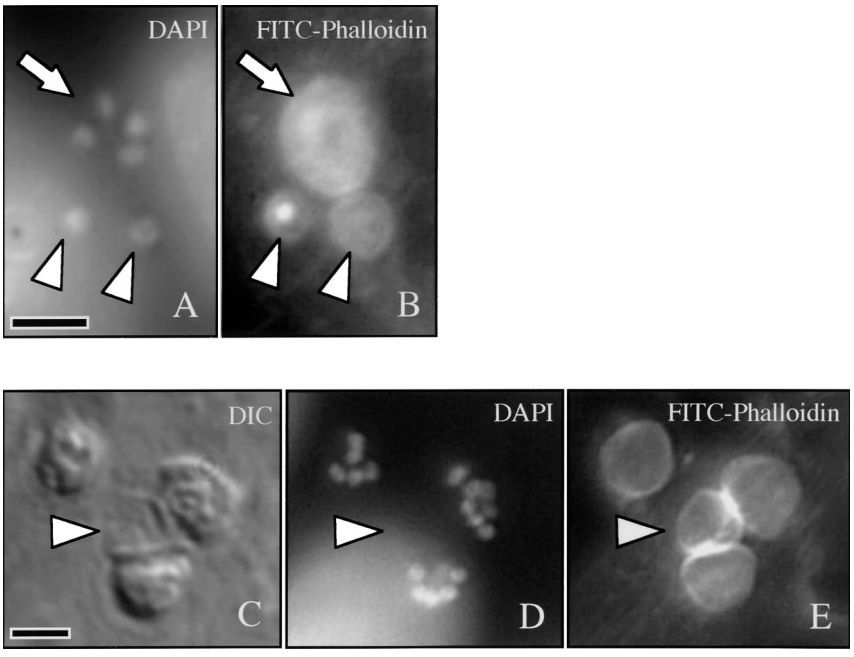

FIG. 2. Fluorescence microscopy of a *Cryptosporidium*-infected cell line stained with DAPI (A) reveals a meront with four nuclei (arrow) and two trophozoites with single nuclei (arrowheads). FITC-phalloidin staining of the same field (B) demonstrates the circular f-actin plaque associated with each parasite. Note the intense central staining of one trophozoite-associated plaque (left arrowhead). A DIC image of another field shows four sites of infection (C), with one parasite removed by exposure to a hypotonic solution (arrowhead). DAPI staining of the same field (D) reveals multiple nuclei within the remaining three parasites. FITC-phalloidin staining of this field (E) demonstrates the circular f-actin plaque associated with each site of invasion, including the site from which the developing parasite was removed (arrowhead). Scale bars = 5 μm.

(Fig. 2E), further arguing for host cell localization of the f-actin. Also, confocal microscopic analysis of longitudinal (*x-z* section) images of FITC-phalloidin-stained infected cells suggested that this f-actin plaque was at the host-parasite interface rather than throughout the parasite (Fig. 3). Several fortuitously identified images of merozoites invading host cells indicated that this actin accumulation was an early event in the invasion process and was initiated before the parasite was entirely internalized (Fig. 4). No other changes in host cell f-actin distribution or organization were detected using these methods.

The *Cryptosporidium*-induced actin plaque is derived from host cell actin. Although the previous results suggested that the f-actin incorporated into the junctional complex was host cell derived, it remained theoretically possible that we were observing an accumulation of *Cryptosporidium* actin at the host-parasite interface. To test the hypothesis that the actin plaque was host cell derived, we designed experiments that used a host cell line (MDCK) constitutively expressing GFP-actin (25). In this cell line, f-actin-containing structures, such as microvilli, stress fibers, and adherens junctions, were easily visualized by fluorescence microscopy (data not shown). Upon infection with *Cryptosporidium*, fluorescent plaques were evident at every site of infection upon fluorescence microscopy, similar to those seen with phalloidin staining and antiactin immunofluorescence microscopy (Fig. 5). Uninfected monolayers displayed no fluorescent plaques. Obviously, the only source of fluorescence in the infected cells is host cell GFP-actin. Indirect immunofluorescence microscopy with anti-GFP antibodies produced similar results (data not shown).

Indirect immunofluorescence microscopy confirms the presence of actin and other actin-associated proteins at the host-parasite interface. Indirect immunofluorescence of a *Cryptosporidium*-infected cell line using antibodies against actin revealed a staining pattern similar to the FITC-phalloidin staining, confirming the previous results (Fig. 6). The staining pattern of extracellular merozoites with this antibody is extremely weak and diffuse (data not shown). Because f-actin organization within cells requires accessory proteins, we per-

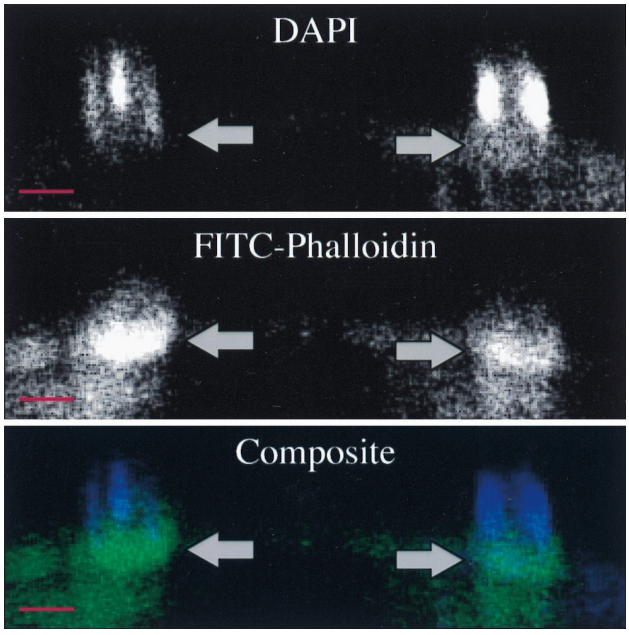

FIG. 3. Confocal laser scanning microscopic longitudinal section through a DAPI- and FITC-phalloidin-stained *Cryptosporidium*-infected cell line demonstrating actin accumulation (arrows and green in composite) at the host-parasite interface, just below the parasite nuclei (blue in composite). The base of the host cell is toward the bottom of each photograph. Scale bars = 5 μm.

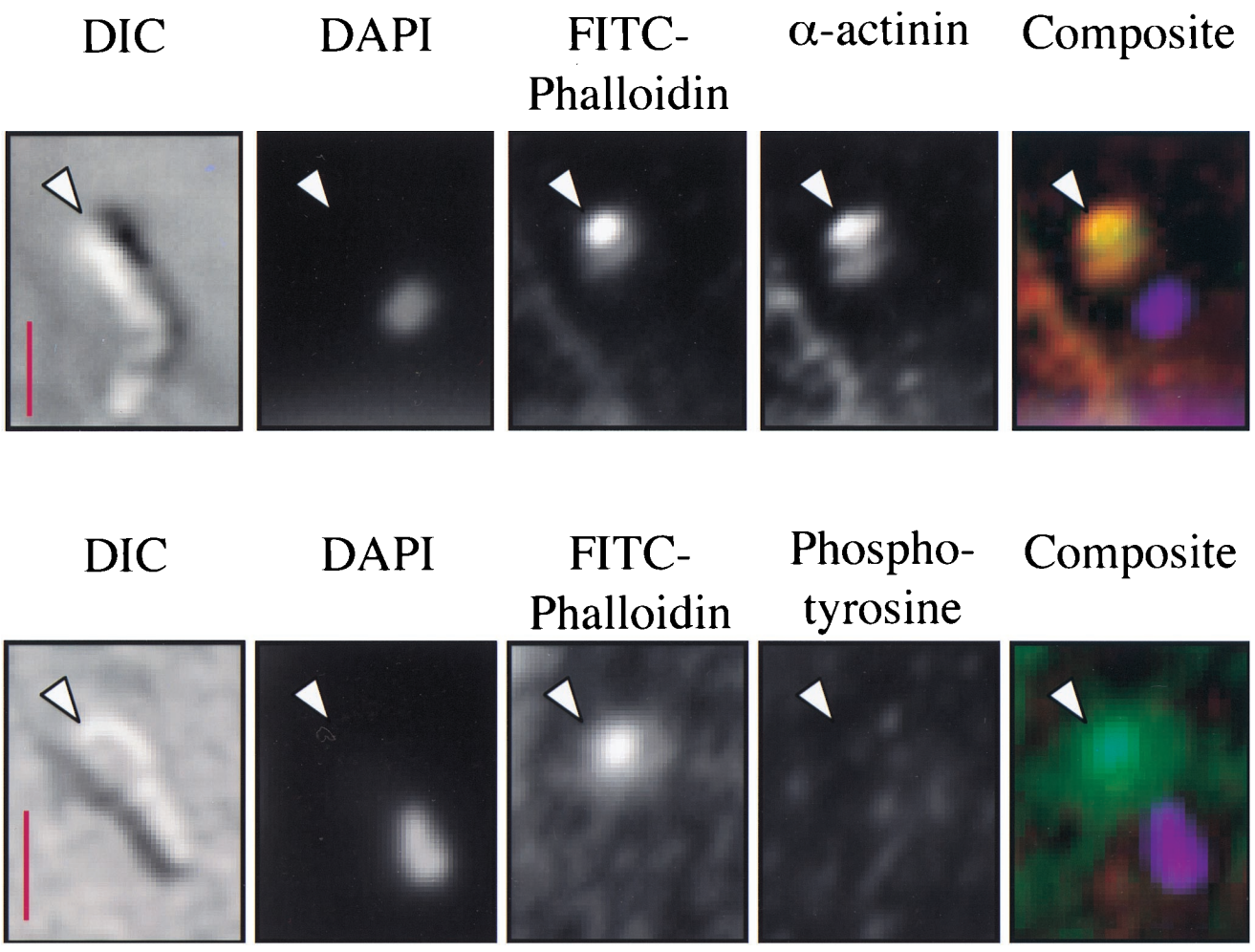

FIG. 4. Fluorescence and DIC microscopy of two *Cryptosporidium* merozoites invading HCT-8 cells. The DIC images show elongated merozoites on the surface of the host cells, with the partially intracellular apical ends of the parasites indicated by arrowheads. The DAPI images of the same fields reveal the single merozoite nucleus toward the posterior end of the parasite. FITC-phalloidin stained f-actin is present at the site of invasion (arrowhead). Indirect immunofluorescence indicates the colocalization of α-actinin with f-actin early in invasion (yellow in composite, upper panel). The anterior portion of extracellular merozoites does not normally intensely express actin or α-actinin (data not shown). Also, there is no evidence of phosphotyrosine at this point of early invasion (lower panel). The basolateral focal adhesions, which are known to contain phosphotyrosine, were clearly positive in these cells (data not shown). Composite image: green, FITC-phalloidin; red, secondary antibody to α-actinin or phosphotyrosine; lavender, DAPI; yellow, colocalization of red and green. Scale bars = 2.5 μm.

formed an indirect immunofluorescence analysis of several actin-associated proteins to better understand the mechanism of f-actin reorganization in infected cells. Indirect immunofluorescence with antibodies against α-actinin, an f-actin-cross-linking protein, revealed striking colocalization of α-actinin with sites of parasite invasion and FITC-phalloidin staining at the trophozoite stage (Fig. 6). Interestingly, later developmental stages (meronts), containing multiple nuclei, entirely lacked staining with this antibody (Fig. 6, insert), suggesting that α-actinin was initially present but was lost (or masked) as the parasite developed. Images of merozoites invading host cells

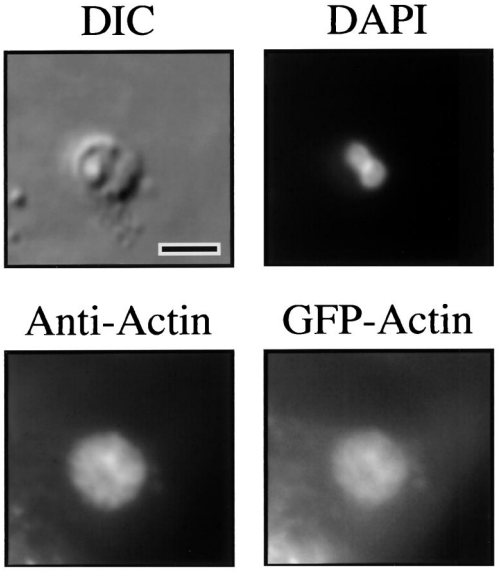

FIG. 5. Fluorescence and DIC microscopy of a *Cryptosporidium*-infected MDCK cells constitutively expressing GFP-actin. The DIC image shows a *Cryptosporidium* meront in the MDCK cell line monolayer. The DAPI image of the same field reveals two nuclei of the parasite. Indirect immunofluorescence of the same field using antiactin antibodies highlights the actin plaque beneath the parasite. Fluorescence microscopy of the same field in the GFP fluorescence range reveals an image identical to the antiactin immunofluorescence, confirming the host cell origin of the actin plaque. Indirect immunofluorescence with anti-GFP antibodies produces identical staining of the actin plaque (data not shown). Scale bar = 5 μm.

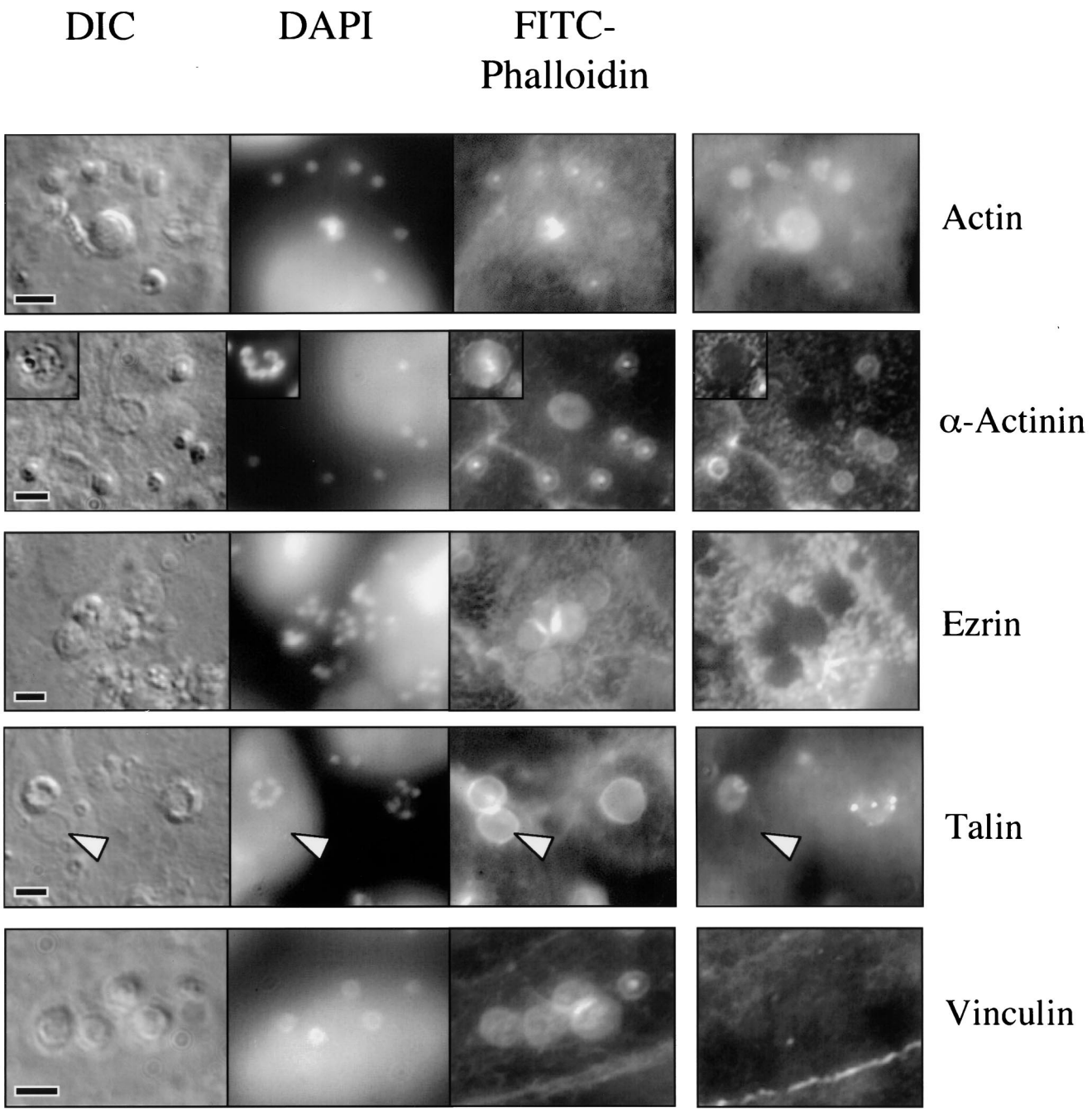

FIG. 6. Indirect immunofluorescence of actin and actin-associated proteins in a *Cryptosporidium*-infected cell line. Photomicrographs of a *Cryptosporidium*-infected cell line reveal DIC images of parasites, parasite nuclei (DAPI), and actin plaques at sites of invasion (FITC-phalloidin). Indirect immunofluorescence using antibodies against actin confirms the presence of actin at each site of invasion in trophozoites (single nuclei) and meronts (center; row 1, column 4). Antibodies against α-actinin (row 2, column 4) reveal the presence of this molecule at sites of developing trophozoites but no staining associated with meronts (insert). Indirect immunofluorescence also shows that ezrin (row 3, column 4) and vinculin (row 5, column 4) are clearly absent from sites of invasion. The linear staining pattern of an adherens junction is shown in the vinculin image (lower right). Although there is some staining by antitalin antibodies (row 4, column 4), the pattern is heterogeneous and is lost when parasites are removed (arrowhead), suggesting that this antibody cross-reacts with the parasite and does not decorate the actin plaque itself. Scale bars = 5 μm.

indicated that α-actinin was present early in the invasion process and colocalized with actin at the site of invasion (Fig. 4). The focal adhesion-associated actin-binding molecules, talin and vinculin, have previously been identified in the host cell actin accumulations associated with enteropathogenic *Escherichia coli* (EPEC), *Salmonella*, and/or *Shigella* infection (12, 13, 30), but these molecules were not identified in the actin plaque (Fig. 6). Although there is some cross-reactivity of the antitalin antibodies with the parasite, this staining is lost when parasites are hypotonically removed. Staining of basolateral focal adhesions within host cells served as an internal positive control. Ezrin, a molecule involved in the cross-linking of f-actin to integral membrane proteins and found in association with adherent EPEC (12), was clearly excluded from the host-

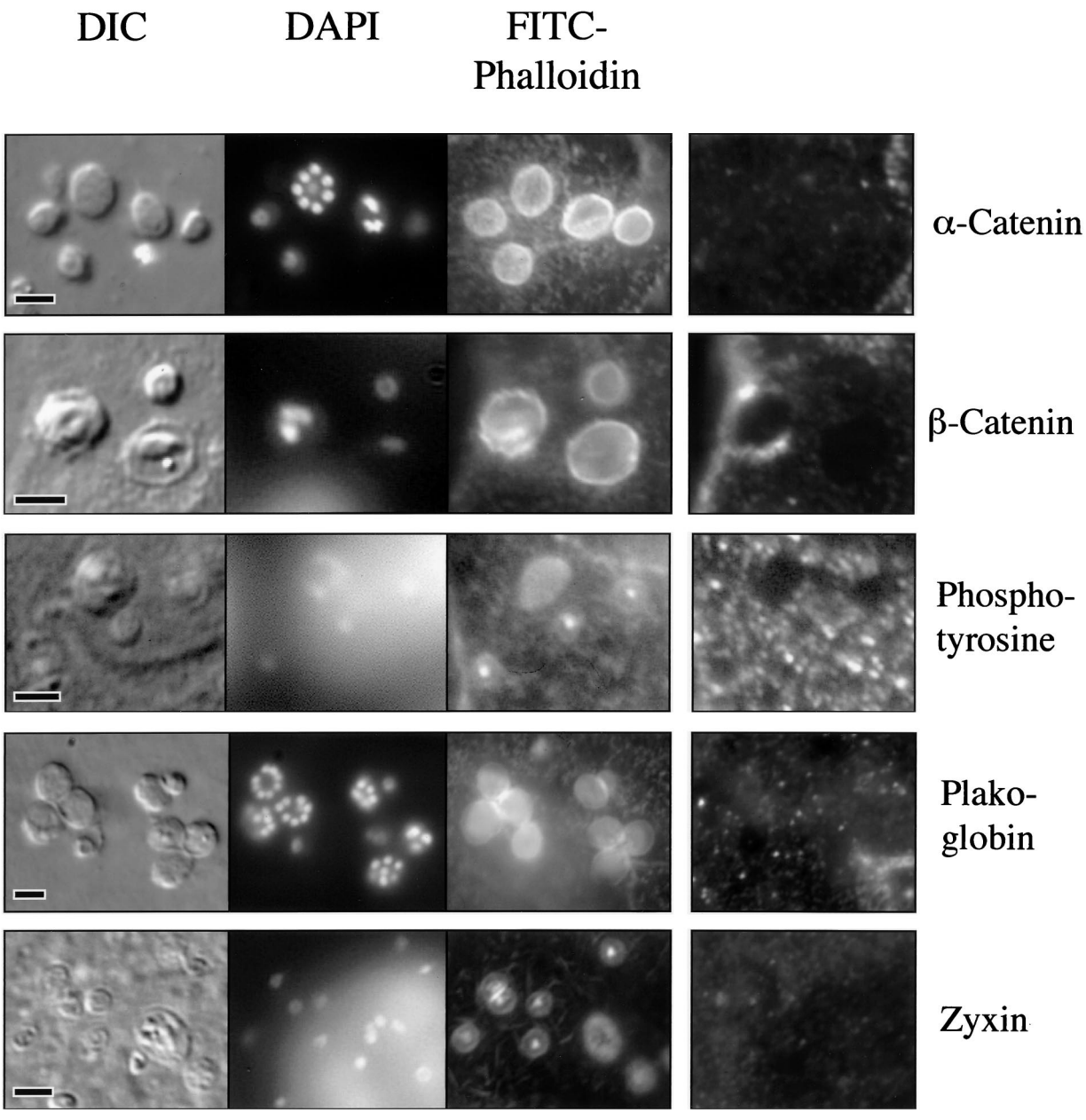

FIG. 7. Indirect immunofluorescence of phosphotyrosine and proteins that link f-actin to membrane in a *Cryptosporidium*-infected cell line. The DIC, DAPI-stained, and FITC-phalloidin-stained images are similar to those described in Fig. 5. Indirect immunofluorescence using antibodies to α-catenin (row 1, column 4), β-catenin (row 2, column 4), phosphotyrosine (row 3, column 4), plakoglobin (row 4, column 4), and zyxin (row 5, column 4), reveal no staining at sites of infection. Internal positive controls (adherens junctions or focal adhesions) were identified for each stain (data not shown). Scale bars = 5 μm.

parasite interface, although it was present in the surrounding cortical region below microvilli (Fig. 6). Indirect immunofluorescence using antibodies against other cytoskeletal components, including vimentin, keratin, villin, and tubulin, failed to identify any obvious rearrangement of these host cell components (data not shown). The villin results are discrepant with those of Forney et al. (14).

The localization of the actin plaque at the host cell membrane suggests that this process may mimic normal cellular structures in which actin is linked to the membrane, such as focal adhesions or adherens junctions. For each of these structures, a multiprotein complex is formed, linking f-actin to a transmembrane protein such as an integrin or E-cadherin (3). Consequently, we examined the actin plaque for evidence of these membrane-linking proteins. The proteins α- and β-catenin and plakoglobin are involved in linking f-actin, via α-actinin, to E-cadherin (1). Our indirect immunofluorescence studies found no evidence of α-catenin, β-catenin, or plakoglobin, or of the focal adhesion-associated protein zyxin, in the region of the actin plaque (Fig. 7) (2). For these studies, the adherens junctions or basolateral focal adhesions found in every cell served as internal positive controls.

Phosphotyrosine-containing proteins have previously been identified in the host cell actin accumulations associated with enteropathogenic bacteria and have been implicated in *Cryptosporidium* invasion by one group (14, 20, 26). As illustrated in

Fig. 7, we were unable to demonstrate phosphotyrosine at the site of developing trophozoites or meronts, despite analysis of numerous parasites. Because tyrosine phosphorylation may represent an early, transient event in the invasion process, we also analyzed several invading merozoites. As shown in Fig. 4, there was no evidence of phosphotyrosine at the site of actin accumulation early in the invasion process. The basolateral focal adhesions in the cell line served as internal positive controls for these studies.

DISCUSSION

The interface between *Cryptosporidium* and the host cell cytoplasm is morphologically unique among protozoan parasites. It is likely to play a structural role in the creation of an intracellular niche for the parasite, but in theory it may also modulate molecular interchange with the host or protect the parasite from host cell defenses. One group has previously found that the antiparasitic drug paromomycin reaches the parasite via the apical membranes overlying the parasite, rather than from the host cell cytoplasm, suggesting exclusion of this molecule from the parasitophorous vacuole (16). Unfortunately, little is known about its composition or the mechanism of its formation. We have found that f-actin and α-actinin are components of this interface complex.

Utilization of host cell actin is a common theme in microbial pathogenesis and has been observed in *E. coli*, *Salmonella*, *Shigella*, and *Listeria* infections (11). Each of these organisms utilizes host actin for a different purpose and employs different mechanisms to recruit and assemble actin microfilaments. In EPEC infections, f-actin forms the scaffolding for a host cell protuberance to which the bacteria attach (12). In *Salmonella* and *Shigella* infections, the actin microfilaments direct the engulfment of the bacteria by the host cell (5, 13). *Listeria* and vaccinia virus nucleate host cell actin on their surfaces to propel themselves through the host cell cytoplasm (6, 8, 27). *Cryptosporidium* appears to utilize f-actin as a structural component of the host-parasite junctional complex. It is also possible that f-actin may play a more active role in the invasion process. Although the related parasite *Toxoplasma gondii* does not require host cell actin for invasion, it does not form the same host-parasite junctional complex as *Cryptosporidium* (9). The role of host cell α-actinin in the *Cryptosporidium* invasion process is not known. α-Actinin binds f-actin and is a known actin-cross-linking protein (10); consequently, it may simply be assembling individual filaments into a larger plaque during *Cryptosporidium* development. It is interesting that the apparent disappearance of α-actinin from the actin plaque after the trophozoite stage of development coincides with the previously described disappearance of a portion of the parasitophorous vacuole membrane adjacent to the actin plaque (21). This suggests that α-actinin may initially link f-actin to a membrane-associated molecule and be shed when the membrane is lost.

Our studies indicate that the actin plaque is a sharply circumscribed aggregation of f-actin that is intimately associated with the host cell plasma membrane, particularly early in the invasion process. Consequently, it appears that *Cryptosporidium* may be mimicking a normal host cell structure that links f-actin to the membrane, such as a focal adhesion complex or an intercellular adherens junction. In each of these molecular complexes, f-actin is linked to an integral membrane protein (E-cadherin or integrins) via an assembly of linker molecules (α- and β-catenin, vinculin, talin, etc.) (1, 3, 17, 23, 24). Our studies did not identify any of these linker molecules, other than α-actinin, in the actin plaque. Consequently, *Cryptosporidium* appears to employ a unique mechanism to organize f-actin at the host-parasite interface.

Recently Forney et al. have also found host cell actin aggregation at the site of *Cryptosporidium* invasion (14). These investigators implied that the observed actin aggregation was due to hypertrophy of host cell microvilli adjacent to the invading parasite. While we and others have occasionally observed such microvillus elongation (29; D. A. Elliott and D. P. Clark, unpublished observations), we have now clearly shown that the observed host cell actin accumulation is a plaque-like accumulation at the host-parasite interface. These investigators have also suggested that tyrosine phosphorylation is an important early event in *Cryptosporidium* invasion. We have not been able to replicate these results. Interestingly, the related parasite *T. gondii* does not utilize tyrosine phosphorylation during the host cell invasion process (22). Additional studies are necessary to address the mechanism of this actin accumulation.

ACKNOWLEDGMENTS

The GFP-actin-expressing MDCK cell line was a generous gift from Angela Barth (Stanford University School of Medicine) and Eugenio de Hostos (University of California, San Francisco). We are indebted to the following individuals for many helpful discussions, technical assistance, and critical reagents: Sue Craig, Doug Murphy, Mike Delanoy, Carol Cooke, Justina Minda, Chip Montrose, Cindy Sears, and Pierre Coulombe. We also thank Sue Craig and Vern Carruthers for reviewing the manuscript.

This work was supported by a grant from the Johns Hopkins Fund for Medical Discovery and a Johns Hopkins Institutional Research Grant. D.P.C. was a recipient of a Merck Clinician-Scientist award.

REFERENCES

1. **Aberle, H., H. Schwartz, and R. Kemler.** 1996. Cadherin-catenin complex: protein interactions and their implications for cadherin function. J. Cell Biochem. **61:**514–523.
2. **Beckerle, M. C.** 1997. Zyxin: zinc fingers at sites of cell adhesion. Bioessays **19:**949–957.
3. **Brugge, J. S.** 1998. Casting light on focal adhesions. Nat. Genet. **19:**309–311.
4. **Clark, D. P., and C. L. Sears.** 1996. The pathogenesis of cryptosporidiosis. Parasitol. Today **12:**221–225.
5. **Clerc, P., and P. J. Sansonetti.** 1987. Entry of *Shigella flexneri* into HeLa cells: evidence for directed phagocytosis involving actin polymerization and myosin accumulation. Infect. Immun. **55:**2681–2688.
6. **Cudmore, S., P. Cossart, G. Griffiths, and M. Way.** 1995. Actin-based motility of vaccinia virus. Nature **378:**636–638.
7. **Current, W. L., and L. S. Garcia.** 1991. Cryptosporidiosis. Clin. Microbiol. Rev. **4:**325–358.
8. **Dabiri, G. A., J. M. Sanger, D. A. Portnoy, and F. S. Southwick.** 1990. *Listeria monocytogenes* moves rapidly through the host-cell cytoplasm by inducing directional actin assembly. Proc. Natl. Acad. Sci. USA **87:**6068–6072.
9. **Dobrowolski, J. M., and L. D. Sibley.** 1996. *Toxoplasma* invasion of mammalian cells is powered by the actin cytoskeleton of the parasite. Cell **34:** 933–939.
10. **Dubreuil, R.** 1991. Structure and evolution of the actin crosslinking proteins. Bioessays **13:**219–226.
11. **Finlay, B. B., and P. Cossart.** 1997. Exploitation of mammalian host cell functions by bacterial pathogens. Science **276:**718–725.
12. **Finlay, B. B., I. Rosenshine, M. S. Donnenberg, and J. B. Kaper.** 1992. Cytoskeletal composition of attaching and effacing lesions associated with enteropathogenic *Escherichia coli* adherence to HeLa cells. Infect. Immun. **60:**2541–2543.
13. **Finlay, B. B., S. Ruschkowski, and S. Dedhar.** 1991. Cytoskeletal rearrangements accompanying *Salmonella* entry into epithelial cells. J. Cell Sci. **99:** 283–296.
14. **Forney, J. R., D. B. DeWald, S. Yang, C. A. Speer, and M. C. Healey.** 1999. A role for host phosphoinositide 3-kinase and cytoskeletal remodeling during *Cryptosporidium parvum* infection. Infect. Immun. **67:**844–852.
15. **Godwin, T. A.** 1991. Crytosporidiosis in the acquired immunodeficiency syndrome: a study of 15 autopsy cases. Hum. Pathol. **22:**1215–1224.
16. **Griffiths, J. K., R. Balakrishnan, G. Widmer, and S. Tzipori.** 1998. Paromomycin and geneticin inhibit intracellular *Cryptosporidium parvum* without trafficking through the host cell cytoplasm: implications for drug delivery. Infect. Immun. **66:**3874–3883.

17. **Jou, T.-S., D. Stewart, J. Stappert, W. Nelson, and J. A. Marrs.** 1995. Genetic and biochemical dissection of protein linkages in the cadherin-catenin complex. Proc. Natl. Acad. Sci. USA **92:**5067–5071.
18. **Lefkowitch, J. H., S. Krumholz, K.-C. Feng-Chen, P. Griffin, D. Despommier, and T. A. Brasitus.** 1984. Cryptosporidiosis of the human small intestine: a light and electron microscopic study. Hum. Pathol. **15:**746–752.
19. **Lumadue, J. A., Y. C. Manabe, R. D. Moore, P. C. Belitsos, C. L. Sears, and D. P. Clark.** 1998. A clinicopathologic analysis of AIDS-related cryptosporidiosis. AIDS **12:**2459–2466.
20. **Manjarrez-Hernandez, H. A., T. J. Baldwin, A. Aitken, S. Knutton, and P. H. Williams.** 1992. Intestinal epithelial cell protein phosphorylation in enteropathogenic *Escherichia coli* diarrhoea. Lancet **339:**521–523.
21. **Marcial, M. A., and J. L. Madara.** 1986. *Cryptosporidium*: cellular localization, structural analysis of absorptive cell-parasite membrane-membrane interactions in guinea pigs, and suggestion of protozoan transport by M cells. Gastroenterology **90:**583–594.
22. **Morisaki, J. H., J. E. Heuser, and L. O. Sibley.** 1995. Invasion of *Toxoplasma* gondii occurs by active penetration of the host cell. J. Cell Sci. **108:**2457–2464.
23. **Nieset, J. E., A. R. Tedfield, F. Jin, K. A. Knudsen, K. R. Johnson, and M. J. Wheelock.** 1997. Characterization of the interactions of alpha-catenin with α-actinin and β-catenin/plakoglobin. J. Cell Sci. **110:**1013–1022.
24. **Ozawa, M., M. Ringwald, and R. Kemler.** 1990. Uvomorulin-catenin complex formation is regulated by a specific domain in the cytoplasmic region of the cell adhesion molecule. Proc. Natl. Acad. Sci. USA **87:**4246–4250.
25. **Robbins, J. R., A. I. Barth, H. Marquis, E. L. de Hostos, W. J. Nelson, and J. A. Theriot.** 1999. *Listeria monocytogenes* exploits normal host cell processes to spread from cell to cell. J. Cell Biol. **146:**1333–1350.
26. **Rosenshine, I., M. S. Donnenberg, J. B. Kaper, and B. B. Finlay.** 1992. Signal transduction between enteropathogenic *Escherichia coli* (EPEC) and epithelial cells: EPEC induces tyrosine phosphorylation of host cell proteins to initiate cytoskeletal rearrangement and bacterial uptake. EMBO J. **11:**3551–3560.
27. **Tilney, L. G., and D. A. Portnoy.** 1989. Actin filaments and the growth, movement, and spread of the intracellular bacterial parasite, *Listeria monocytogenes*. J. Cell Biol. **109:**1597–1608.
28. **Tzipori, S., and J. K. Griffiths.** 1998. Natural history and biology of *Cryptosporidium parvum*. Adv. Parasitol. **40:**6–36.
29. **Vetterling, J. M., A. Takeuchi, and P. A. Madden.** 1971. Ultrastructure of *Cryptosporidium wrairi* from the guinea pig. J. Protozool. **18:**248–260.
30. **Watarai, M., Y. Kamata, S. Kozaki, and C. Sasakawa.** 1997. Rho, a small GTP-binding protein, is essential for *Shigella* invasion of epithelial cells. J. Exp. Med. **185:**281–292.

Editor: T. R. Kozel